LA-UR- 08-4807

Approved for public release; distribution is unlimited.

Title:	Mesoscopic Modeling of Liquid Water Transport in Polymer Electrolyte Fuel Cells
Author(s):	Partha P. Mukherjee Chao-Yang Wang
Intended for:	Paper for the PEM Fuel Cells Proceedings, PRIME, 214th Electrochemical Society Meeting, Honolulu, HI, October 12-17, 2008

Form 836 (7/06)

Mesoscopic Modeling of Liquid Water Transport in Polymer Electrolyte Fuel Cells

P. P. Mukherjee[a,b], and C. Y. Wang[a]

[a] Electrochemical Engine Center, Department of Mechanical & Nuclear Engineering, Pennsylvania State University, University Park, Pennsylvania 16802, USA
[b] Present address: Los Alamos National Laboratory, Mail Stop T003, Los Alamos, New Mexico 87545, USA

A key performance limitation in polymer electrolyte fuel cells (PEFC), manifested in terms of mass transport loss, originates from liquid water transport and resulting flooding phenomena in the constituent components. Liquid water leads to the coverage of the electrochemically active sites in the catalyst layer (CL) rendering reduced catalytic activity and blockage of the available pore space in the porous CL and fibrous gas diffusion layer (GDL) resulting in hindered oxygen transport to the active reaction sites. The cathode CL and the GDL therefore play a major role in the mass transport loss and hence in the water management of a PEFC. In this article, we present the development of a mesoscopic modeling formalism coupled with realistic microstructural delineation to study the profound influence of the pore structure and surface wettability on liquid water transport and interfacial dynamics in the PEFC catalyst layer and gas diffusion layer.

Introduction

In recent years, the polymer electrolyte fuel cell (PEFC) has emerged as a promising power source for a wide range of applications. Despite tremendous recent progress in enhancing the overall cell performance, a pivotal performance limitation in PEFCs centers on liquid water transport and resulting flooding in the constituent components (1). Liquid water blocks the porous pathways in the CL and GDL thus causing hindered oxygen transport to the reaction sites as well as covers the electrochemically active sites in the CL thereby increasing surface overpotential. This phenomenon is known as "flooding" and is perceived as the primary mechanism leading to the limiting current behavior in the cell performance. The catalyst layer and gas diffusion layer, therefore, play a crucial role in the PEFC water management (1) aimed at maintaining a delicate balance between reactant transport from the gas channels and water removal from the electrochemically active sites. In the last few years, water management research has received wide attention, evidenced by the development of several macroscopic models for liquid water transport in PEFCs (2-6). The macroscopic models for liquid water transport, reported in the literature, are based on the theory of volume averaging and treat the catalyst layer and gas diffusion layer as macrohomogeneous porous layers. Due to the macroscopic nature, the current models fail to resolve the influence of the structural morphology of the CL and GDL on the underlying two-phase dynamics. Although substantial research, both modeling and experimental, has been conducted to study flooding and water transport in PEFCs, there is serious paucity of fundamental understanding regarding the overall structure-wettability-transport interactions as well as underlying two-phase dynamics in the catalyst layer and the gas diffusion layer.

In this article, the development of a mesoscopic two-phase lattice Boltzmann model coupled with stochastic microstructure reconstruction technique for the CL and GDL of a PEFC is presented in order to gain fundamental insight into the structure-wettability influence on the underlying liquid water transport and interfacial dynamics.

Model and Theory

The modeling approach comprises of a stochastic reconstruction method for the generation of the CL and GDL microstructures and a two-phase lattice Boltzmann method for studying liquid water transport through the reconstructed microstructures.

Microstructure Reconstruction

In this work, we have developed stochastic reconstruction techniques for the generation of CL and GDL microstructures. The catalyst layer is delineated as a two-phase (pore/solid) structure consisting of the gas phase (i.e. the void space) and a mixed electrolyte/electronic phase (i.e. the solid matrix), which can be well justified from the uniform electronic potential arising from the highly conductive electronic (C and Pt) phase (7). The gas diffusion layer is considered as a non-woven fibrous structure e.g. carbon paper.

The stochastic reconstruction method for the CL microstructure generation is based on the idea that an arbitrarily complex porous structure can be described by a binary phase function which takes the value 0 in the pore space and 1 in the solid space. The inherently random description of the Gaussian distribution is qualified by the porosity and two-point autocorrelation function, which generates the 3D description of the porous medium as the binary phase function. This method for reconstructing the CL microstructure is detailed in Ref. (7). The stochastic reconstruction method for the fibrous structure generation of a non-woven carbon paper GDL is based on a Poisson line process with one-parametric directional distribution where the fiber diameter and shape distribution are be selected according to the GDL fabrication specifications (8). The details of the non-woven GDL structure generation method are furnished in Ref. (8). Figure 1 shows representative 3D reconstructed microstructures of the PEFC catalyst layer and gas diffusion layer.

Two-Phase Lattice Boltzmann Model

In recent years, the lattice Boltzmann (LB) method, owing to its excellent numerical stability and constitutive versatility, has developed into a powerful technique for simulating fluid flows and is particularly successful in fluid flow applications involving interfacial dynamics and complex geometries (9). The LB method is a first-principle based numerical approach. Unlike the conventional Navier-Stokes solvers based on the discretization of the macroscopic continuum equations, lattice Boltzmann methods consider flows to be composed of a collection of pseudo-particles residing on the nodes of an underlying lattice structure which interact according to a velocity distribution function. The lattice Boltzmann method is also an ideal scale-bridging numerical scheme which incorporates simplified kinetic models to capture microscopic or mesoscopic flow physics and yet the macroscopic averaged quantities satisfy the desired macroscopic equations (9).

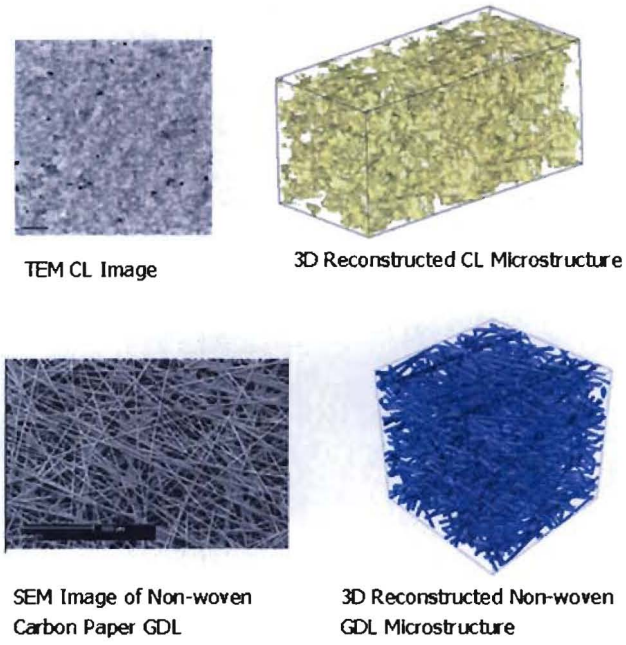

Figure 1. 3D reconstructed CL and GDL microstructures along with 2D SEM/TEM images.

The two-phase lattice Boltzmann model developed in this work is based on the interaction potential model, originally proposed by Shan and Chen (10). This model introduces k distribution functions for a fluid mixture comprising of k components. Each distribution function represents a fluid component and satisfies the evolution equation. The non-local interaction between particles at neighboring lattice sites is included in the kinetics through a set of potentials. The LB equation for the kth component can be written as:

$$f_i^k(\mathbf{x}+\mathbf{e}_i\delta_t, t+\delta_t) - f_i^k(\mathbf{x},t) = -\frac{f_i^k(\mathbf{x},t) - f_i^{k(eq)}(\mathbf{x},t)}{\tau_k} \qquad [1]$$

where $f_i^k(\mathbf{x},t)$ is the number density distribution function for the kth component in the ith velocity direction at position $\mathbf{x}$ and time t, and δ_t is the time increment. In the term on the right-hand side, τ_k is the relaxation time of the kth component in lattice unit, and $f_i^{k(eq)}(\mathbf{x},t)$ is the corresponding equilibrium distribution function. The right-hand-side of Eq. [1] represents the collision term, which is simplified to the equilibrium distribution function $f_i^{k(eq)}(\mathbf{x},t)$ by the so-called BGK (Bhatnagar-Gross-Krook), or the single-time relaxation approximation (11). A three-dimensional 19-speed lattice (D3Q19, where D is the dimension and Q is the number of velocity directions) is used in the model. Surface tension between the two phases is realized through a fluid/fluid interaction force and the wall adhesion effect i.e. the contact angle is incorporated via a fluid/solid interaction force. The details of the two-phase lattice Boltzmann model developed for this study are furnished in Ref. (10,12,13).

Two-Phase Numerical Experiments

In this study, two numerical experiments are specifically designed for investigating liquid water transport and two-phase dynamics through the reconstructed CL and GDL microstructures. Before describing the details of the numerical experiments, it is important to mention that the two-phase transport in the PEFC CL and GDL is characterized by capillary transport as evidenced by very low Capillary number (Ca = $\frac{\mu_2 U_2}{\sigma} \sim 10^{-6}$) operation. In the Capillary number expression, U_2 and μ_2 are the non-wetting phase Darcy velocity and dynamic viscosity respectively, σ is the surface tension. In the capillary transport regime, surface forces dominate over the inertial, viscous and gravity forces (13).

The first numerical setup is devised to simulate a *quasi-static displacement experiment*, detailed elsewhere in the literature (14), for simulating immiscible, two-phase transport through the CL and GDL structures. A non-wetting phase (NWP) reservoir is added to the porous structure at the front end and a wetting phase (WP) reservoir is added at the back end (13). It should be noted that for the *primary drainage* (PD) simulation in the hydrophobic CL and GDL, liquid water is the NWP and air is the WP. The primary drainage process is simulated starting with zero capillary pressure, by fixing the NWP and WP reservoir pressures to be equal. Then the capillary pressure is increased incrementally by decreasing the WP reservoir pressure while maintaining the NWP reservoir pressure at the fixed initial value. The pressure gradient drives liquid water into the initially air-saturated CL and GDL by displacing it. The details about the numerical setup corresponding to the primary drainage simulation are furnished in Ref. (13). The primary objective of the quasi-static displacement simulation is to study the liquid water behavior through the porous CL and fibrous GDL structures and the concurrent response to capillarity as a direct manifestation of the underlying pore-morphology.

In order to have enhanced fundamental insight into the underlying two-phase transport and interfacial dynamics, another numerical experiment is designed based on the *steady-state flow experiment*, typically devised in the petroleum/reservoir engineering applications and detailed elsewhere in the literature (14). Briefly, in the steady-state flow experiment the two immiscible fluids are allowed to flow simultaneously until equilibrium is attained and the corresponding saturations, fluid flow rates and pressure gradients can be directly measured and correlated using Darcy's law. In the *steady-state flow simulation*, initially both the NWP and WP are randomly distributed throughout the CL and GDL porous structures such that the desired NWP saturation is achieved. The initial random distribution of the liquid water phase (i.e. NWP) in the otherwise air (i.e. WP) occupied CL closely represents the physically perceived scenario of liquid water generation due to the electrochemical reaction at different catalytically active sites within the CL structure and subsequent transport by the action of capillarity. Furthermore, in the case of conventional catalyst layers characterized by low hydrophobicity, liquid water generated in the CL fails to overcome the capillary pressure barrier imposed by the sufficiently hydrophobic microporous layer (MPL) situated between the CL and GDL. In this scenario, water vapor transports into the GDL and condenses into liquid water at several preferential sites throughout the GDL which subsequently transports due to the action of capillarity (15). These two scenarios form the basis for the present dynamical equilibrium immiscible flow simulation. The details about the numerical setup corresponding to the primary drainage simulation are furnished in Ref. (13).

Results and Discussion

Figure 2 displays the steady state invading liquid water fronts corresponding to increasing capillary pressures from the *primary drainage simulation* in the reconstructed CL characterized by hydrophobic wetting characteristics with a static contact angle of 110^0. At lower capillary pressures, the liquid water saturation front exhibits finger like pattern, similar to the displacement pattern observed typically in the capillary fingering regime. The displacing liquid water phase penetrates into the body of the resident wetting phase (i.e. air) in the shape of fingers owing to the surface tension driven capillary force. However, at high saturation levels, the invading non-wetting phase tends to exhibit a somewhat flat advancing front. This observation indicates that with increasing capillary pressure, even at very low Capillary number (Ca), several penetrating saturation fronts tend to merge and form a stable front and the invasion pattern transitions from the capillary fingering regime to the stable displacement regime and might lie in the transition zone in between.

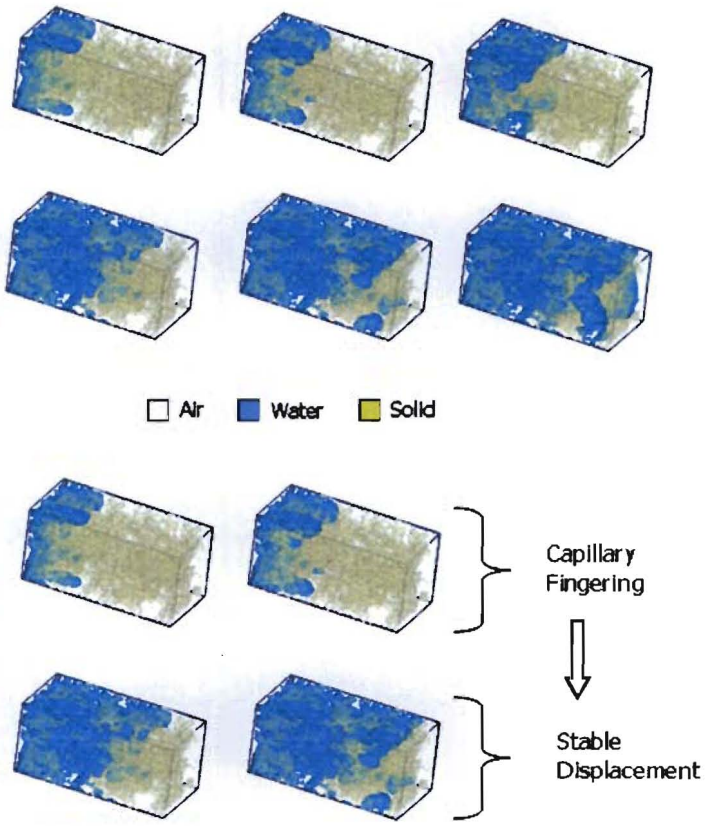

Figure 2. Advancing liquid water front with increasing capillary pressure through the initially air-saturated reconstructed CL microstructure from the primary drainage simulation.

Figure 3 shows the invading liquid water distribution from the *primary drainage simulation* with increasing capillary pressure in the initially air-saturated reconstructed carbon paper GDL characterized by hydrophobic wetting characteristics with a static contact angle of 140^0. For this two-phase simulation, a reconstructed GDL structure with 100^3 lattice points is used keeping in mind the computational overhead in lattice

Boltzmann simulations. At the initially very low capillary pressure, the invading front overcomes the barrier pressure only at some preferential locations depending upon the pore size along with the emergence of droplets owing to strong hydrophobicity. As the capillary pressure increases, several liquid water fronts start to penetrate into the air occupied domain. Further increase in capillary pressure exhibits growth of droplets at two invasion fronts, followed by the coalescence of the drops and collapsing into a single front. This newly formed front then invades into the less tortuous in-plane direction. Additionally, emergence of tiny droplets and subsequent growth can be observed in the constricted pores in the vicinity of the inlet region primarily due to strong wall adhesion forces from interactions with highly hydrophobic fibers with the increasing capillary pressure. One of the several invading fronts reaches the air reservoir at one location corresponding to the capillary pressure.

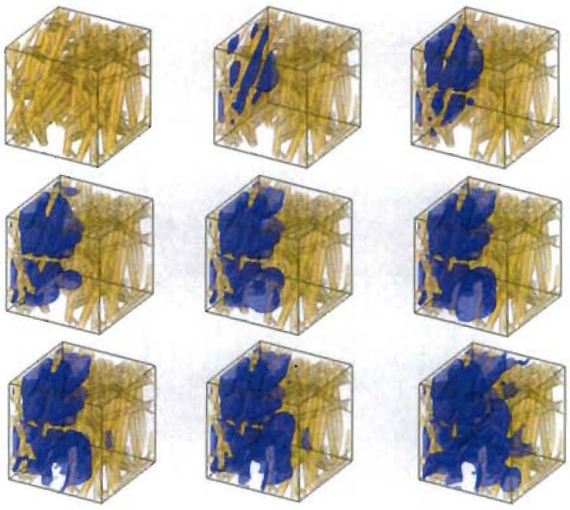

Figure 3. Advancing liquid water front with increasing capillary pressure through the initially air-saturated reconstructed GDL microstructure from the primary drainage simulation.

Figure 4 exhibits the 3D liquid water distributions corresponding to several low saturation levels (below 15%) for the CL from the *steady state flow simulation* at equilibrium. It can be observed that below 10% saturation level there is hardly any connected pathway for the liquid water phase to transport through the CL structure and hence the relative mobility of the liquid water phase with respect to the incumbent air phase is negligible. As the saturation level increases the initially random liquid water phase redistributes owing to the action of capillarity and finds a connected pathway for transport through the CL structure. From this simulation, the relative permeability, a key two-phase parameter, can be evaluated as a function of liquid water saturation pertaining to the interfacial interactions and pore morphology of the CL structure.

Figure 5 shows the equilibrium liquid water distribution after the randomly dispersed initial liquid water redistributes by the action of capillary force for a purely hydrophobic GDL with contact angle of around 140^{o} and also for a mixed wettability GDL with hydrophilic and hydrophobic contact angles of 80^{o} and 140^{o}, respectively. In the mixed wettability GDL, a hydrophilic pore fraction of 50% is considered and the hydrophilic pores are assumed to be randomly distributed through the GDL structure.

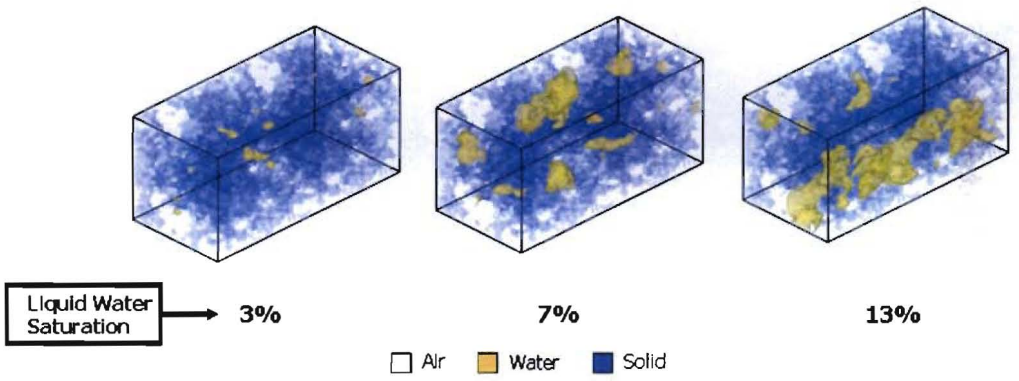

Figure 4. 3D liquid water distributions in the reconstructed CL microstructure from the steady state flow simulation at equilibrium.

It can be observed that at similar saturation level, the liquid water distribution is quite different for the two GDLs, underscoring the influence of the wetting characteristics and interfacial dynamics on transport processes. In a mixed wettability GDL, due to the hydrophilic pores, liquid water exhibits a somewhat stable front preferentially oriented along the through-plane direction. On the other hand, in a purely hydrophobic GDL, liquid water tends to distribute preferentially in the less tortuous in-plane direction and exhibits a narrow flooding front, which would facilitate effective oxygen transport along the through-plane direction from the gas channels to the CL active sites. Finally, it is worth pointing out that the two-phase lattice Boltzmann (LB) model not only captures the pore occupancy by liquid water due to pore size distribution but also phase redistribution owing to the underlying interfacial dynamics and wetting characteristics.

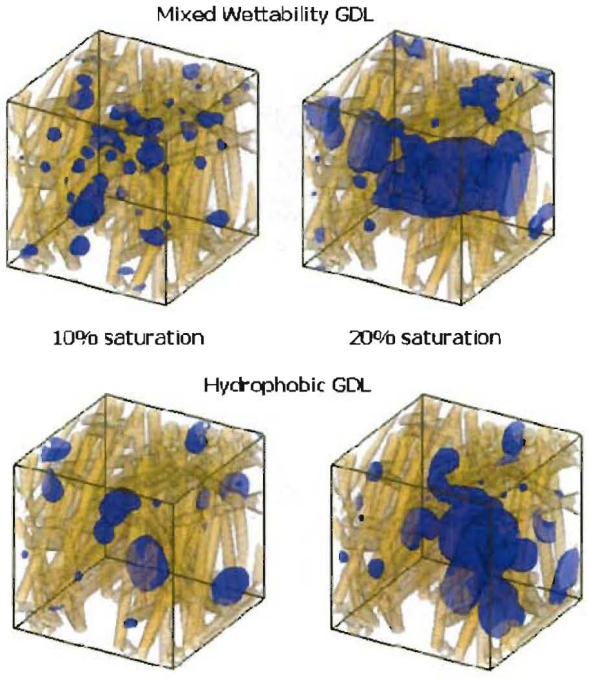

Figure 5. 3D liquid water distributions in a hydrophobic and a mixed wettability GDL from the two-phase LB simulations.

Conclusions

The catalyst layer and the gas diffusion layer play a crucial role in the overall PEFC performance due to the transport limitation in the presence of liquid water and flooding phenomena. In this work, the development of a mesoscopic, two-phase lattice Boltzmann model coupled with a stochastic microstructure reconstruction model is presented in order to reveal the structure-wettability influence on the underlying liquid water transport and flooding dynamics in the PEFC CL and GDL. The liquid water flooding front in the CL apparently tends to exhibit a transition from capillary fingering to somewhat stable displacement pattern even in a strictly capillary dominated flow regime. The liquid water transport in the fibrous GDL shows intricate interfacial dynamics including droplet interactions, flooding front formation and propagation. The influence of partially wetting pore structure on the flooding behavior is elucidated for a mixed wettability GDL.

Acknowledgments

PPM would like to thank V. P. Schulz, A. Wiegmann and J. Becker from Fraunhofer ITWM, Germany for collaboration with GDL structure generation. Financial support from NSF through grant No. 0609727 and ECEC industrial sponsors is gratefully acknowledged.

References

1. C. Y. Wang, *Chem. Rev.*, (*Washington, DC*), **104**, 4727 (2004).
2. U. Pasaogullari and C. Y. Wang, *J. Electrochem. Soc.*, **151**, 399 (2004).
3. Y. Wang and C. Y. Wang, *J. Electrochem. Soc.*, **153**, A1193 (2006).
4. A. Z. Weber and J. Newman, *J. Electrochem. Soc.*, **152**, A677 (2005).
5. J. Nam and M. Kaviany, *Int. J. Heat Mass Transfer*, **46**, 4595 (2003).
6. W. He, J. S. Yi, and T. V Nguyen, *AIChE J.*, **46**, 2053 (2000).
7. P. P. Mukherjee and C. Y. Wang, *J. Electrochem. Soc.*, **153**, A840 (2006).
8. V. P. Schulz, J. Becker, A. Wiegmann, P. P. Mukherjee, and C. Y. Wang, *J. Electrochem. Soc.*, **154**, B419 (2007).
9. S. Chen and G. D. Doolen, *Ann. Rev. Fluid Mech.*, **30**, 329 (1998).
10. X. Shan and H. Chen, *Phys. Rev. E*, **47**, 1815, 1993.
11. P. Bhatnagar, E. Gross, and M. Krook, *Phys. Rev.*, **94,** 511 (1954).
12. Q. Kang, D. Zhang, and S. Chen, *J. Fluid Mech.*, **545**, 41 (2005).
13. P. P. Mukherjee, *PhD Dissertation*, Pennsylvania State University, University Park, PA, USA (2007).
14. J. Bear, *Dynamics of Fluids in Porous Media*, Dover, New York (1972).
15. P. K. Sinha, P. P. Mukherjee, and C. Y. Wang, *J. Mater. Chem.*, **17**, 3089 (2007).